American Journal of Civil Engineering and Constructions (AJCEC)

ISSN: 3070-0884 (ONLINE)

VOLUME 2 ISSUE 2 (2026)

PUBLISHED BY
E-PALLI PUBLISHERS, DELAWARE, USA

American Journal of
Civil Engineering and Constructions (AJCEC)

Volume 2 Issue 2, Year 2026
ISSN: 3070-0884 (Online)
DOI: https://doi.org/10.54536/ajcec.v2i2.8444
https://journals.e-palli.com/home/index.php/ajcec

Application of Rice Husk Ash-Derived Nano-Silica as a Partial Replacement of Portland Limestone Cement: Effects on Workability, Compressive Strength, and Mass Gain of Concrete

Adebola Saheed Akolade[1*], Oluwatobiloba Dave Akintayo[1], Oluwatunmise Peter Abolarin[1], John Kehinde Adebayo[1], Precious Adesope Olaomotito[1], Abdulmoruf Olasile Akinsanya[1]

Article Information

Received: June 10, 2026

Accepted: August 27, 2026

Published: September 19, 2026

Keywords

Cement Replacement, Compressive Strength, Nano-Silica, Portland Limestone Cement, Rice Husk Ash

ABSTRACT

Rice husk ash (RHA) is a widely available agricultural waste with potential as a precursor for nano-silica, offering a supplementary cementitious material for concrete production. This study investigated the effect of nano-silica synthesised from RHA, calcined at 600 °C, as a partial replacement for Portland Limestone Cement (PLC) on the workability, compressive strength, and mass gain of concrete at 0%, 4%, and 8% replacement levels. The constituent fine and coarse aggregates were characterised for moisture content, specific gravity, and particle-size distribution before concrete production, and confirmed suitable for normal-weight concrete. Workability decreased progressively with increasing nano-silica content, with slump values dropping from 60 mm for the control mix to 45 mm and 35 mm at 4% and 8% replacement, respectively, although values remained within a workable range. The curing-period mass increase - measured here as the percentage increase in specimen mass between demoulding and the end of curing, and reported as a study-specific indicator distinct from standardised water absorption - was lowest at 4% replacement (0.66%), against 0.92% for the control and 0.71% at 8% replacement. The 8% replacement achieved the highest 28-day compressive strength, at 21.34 MPa, compared with 18.99 MPa at 4% replacement and 15.55 MPa for the control, associated with the combined filler, nucleation, and pozzolanic effects of nano-silica. Within the replacement levels investigated, 4% replacement provided the best overall balance of workability, compressive strength, and mass gain, while 8% replacement is better suited to applications where maximum 28-day compressive strength is the governing requirement. The findings demonstrate the potential of RHA-derived nano-silica as a supplementary cementitious material for PLC concrete, while providing a route for agricultural-waste valorization.

INTRODUCTION

Concrete remains among the most widely used construction materials globally because of its versatility, compressive strength, durability, and adaptability to different structural forms. Its principal binder, Portland cement, is however associated with a substantial share of global anthropogenic CO_2 emissions, arising mainly from limestone calcination and the combustion of fuel required to attain clinkering temperatures (International Energy Agency [IEA], 2023). Even after accounting for the partial re-absorption of CO_2 by cement materials through carbonation over their service life, cement production remains a significant net contributor to industrial emissions (Wu *et al.*, 2024). These concerns have intensified interest in supplementary cementitious materials (SCMs) that can partially replace cement while maintaining or improving concrete performance (Park *et al.*, 2021; Razzazan *et al.*, 2025). Portland Limestone Cement (PLC), which reduces clinker content by partially replacing it with ground limestone, offers a first step toward lowering the embodied carbon of cement, but researchers continue to explore SCMs capable of replacing cement further without compromising performance (Arvizu-Montes *et al.*, 2025).

Rice husk, an abundant agricultural by-product in rice-producing regions such as Nigeria, yields on controlled combustion an ash rich in amorphous silica, typically containing between 85% and 97% SiO_2, with its pozzolanic reactivity governed principally by combustion temperature and resulting particle fineness (Sawasdee & Pisutpaisal, 2022; Endale *et al.*, 2023). The valorisation of rice husk and other agricultural residues into value-added materials also provides an opportunity to reduce waste while developing materials for sustainable engineering applications (Akolade *et al.*, 2026). A comprehensive review by Barbhuiya *et al.* (2025) found that RHA, incorporated into concrete as a partial cement replacement, consistently enhances compressive strength and improves resistance to chloride ingress, sulphate attack, and carbonation at appropriate replacement levels. When further processed into nano-silica through alkaline extraction and controlled acid precipitation, RHA becomes a substantially more reactive pozzolanic material, with reported extraction routes achieving silica purities in excess of 95% and particle sizes between approximately 14 and 80 nm (Dhaneswara *et al.*, 2020; Ebnalwaled & Almalki, 2022). Such nano-silica is reported to influence cement hydration through combined filler, nucleation, and pozzolanic effects (Anto *et al.*, 2022; Xu *et al.*, 2022), offering a pathway to convert an agricultural

[1] Department of Civil Engineering, Faculty of Engineering and Technology Lead City University, Ibadan, Nigeria
[*] Corresponding author's email: akolade.adebola@lcu.edu.ng

waste stream into a technically valuable construction input while simultaneously addressing waste management and the sustainability of cement-based construction (Indumathi *et al.*, 2024; Xi *et al.*, 2023). Related research has also demonstrated the feasibility of incorporating agricultural-residue-derived materials into cement-bonded construction products, further supporting the potential of waste valorisation in sustainable construction (Akolade *et al.*, 2025).

Previous studies have examined RHA-derived silica and nano-silica in cementitious systems largely using Ordinary Portland Cement (OPC) as the base binder (Anto *et al.*, 2022; Tran *et al.*, 2021). Comparatively limited research has examined the performance of such materials in combination with PLC — a cement variety increasingly specified in construction because of its own reduced embodied carbon (Indumathi *et al.*, 2024). Because PLC already contains a proportion of finely ground limestone that contributes its own filler and nucleation effects, nano-silica derived from RHA is expected to act synergistically with the limestone fraction, with the limestone providing early nucleation and carboaluminate formation while nano-silica sustains pozzolanic consumption of calcium hydroxide into later curing ages, a synergy demonstrated for limestone–RHA systems by Wang *et al.* (2024). Whether this synergy can be relied upon at low, practically relevant replacement levels, and at what dosage this occurs without inducing complications such as particle agglomeration or excessive water demand, remains inadequately resolved: reported optimum nano-silica or microsilica replacement levels vary considerably across studies, from below 1% in some formulations to over 15% in others, depending on the extraction route, particle fineness, and base cement used (Raji *et al.*, 2024; Ullah *et al.*, 2025).

This study addresses these gaps by synthesising nano-silica from locally sourced RHA and evaluating its use as a partial replacement for PLC at 0%, 4%, and 8% replacement levels. The specific objectives were to

- Determine the physical properties of the fine and coarse aggregates used in the concrete mixtures;
- Evaluate the effect of nano-silica incorporation on the fresh properties (workability) of concrete;
- Assess the compressive strength and mass gain of the resulting concrete at 7, 14, and 28 days;
- Compare the modified mixes against an unmodified control to identify the replacement level offering the best overall balance of workability, compressive strength, and mass gain.

The findings are intended to contribute experimental data supporting the use of agricultural-waste-derived nano-silica as a supplementary cementitious material for PLC concrete production.

LITERATURE REVIEW

Nano-Silica as a Supplementary Cementitious Material

Nano-silica (nano-SiO_2) is an ultrafine, amorphous form of silicon dioxide characterised by a very high specific surface area. When incorporated into cementitious materials, nano-silica can influence cement hydration and the resulting microstructure through three complementary mechanisms: the filler effect, the nucleation effect, and the pozzolanic effect. The filler effect occurs because the extremely fine particles physically occupy microscopic voids between cement grains, thereby contributing to paste densification. The nucleation effect results from the large surface area of nano-silica, which provides numerous sites for the precipitation of hydration products and can accelerate early hydration and strength development. The pozzolanic effect involves the reaction of amorphous silica with calcium hydroxide released during the hydration of C_3S and C_2S, producing additional secondary calcium silicate hydrate (C–S–H) gel (Al-Saffar *et al.*, 2023; Xu *et al.*, 2022). These mechanisms can contribute to densification of the interfacial transition zone between the cement paste and aggregate, which is normally more porous and weaker than the bulk cement paste (Xu *et al.*, 2022).

The high specific surface area that makes nano-silica highly reactive also introduces practical challenges. Nano-silica can increase water demand and consequently reduce concrete workability when the water-to-binder ratio is maintained constant. Inadequate dispersion may also promote particle agglomeration at higher replacement levels, reducing the efficiency of particle dispersion and limiting the pore-filling benefits of the material (Farokhzad & Divandari, 2021; Tran *et al.*, 2021). Consequently, the beneficial effects of nano-silica are generally associated with relatively low replacement levels, with reported effective dosages commonly ranging from approximately 1% to 8% by mass of cement (Anto *et al.*, 2022; Ullah *et al.*, 2025).

Rice husk ash (RHA) represents an important precursor for silica-based supplementary cementitious materials because controlled combustion of rice husk produces an ash rich in amorphous silica. The silica content of RHA has been reported to range approximately between 85% and 97%, although its pozzolanic reactivity depends strongly on combustion temperature and particle fineness (Sawasdee & Pisutpaisal, 2022; Endale *et al.*, 2023). The utilisation of RHA-derived materials in cementitious systems therefore provides a potential route for agricultural-waste valorisation while reducing reliance on conventional cementitious materials.

Previous studies have demonstrated the potential of RHA and nano-silica to improve the mechanical and durability performance of cement-based materials. Barbhuiya *et al.* (2025), for example, reported that RHA incorporated at appropriate replacement levels can enhance compressive strength and resistance to chloride ingress, sulphate attack, and carbonation. Further processing of RHA through alkaline extraction and controlled acid precipitation can produce highly reactive silica, with published studies reporting silica purities exceeding 95% and particle sizes in the nanometre range (Dhaneswara *et al.*, 2020;

Ebnalwaled & Almalki, 2022). Nano-silica produced from RHA has consequently attracted attention as a means of combining agricultural-waste management with the development of higher-value construction materials.

RHA-Derived Nano-Silica

Rice husk is an abundant agricultural by-product that can serve as a low-cost precursor for silica production. Under controlled combustion conditions, the organic components of rice husk are removed while much of the silica is retained in the resulting ash. The characteristics of the resulting silica depend strongly on the treatment conditions, particularly the combustion temperature and subsequent chemical extraction process (Sawasdee & Pisutpaisal, 2022).

Wet-chemical extraction and precipitation routes have been widely reported for the production of amorphous silica from RHA. These processes generally involve chemical pretreatment to remove metallic impurities, controlled combustion to produce silica-rich ash, alkaline extraction to dissolve silica as soluble silicate, and acidification to precipitate silica. Dhaneswara *et al.* (2020) investigated the synthesis of amorphous silica from RHA using different acidification methods and alkaline concentrations, while Aprilia *et al.* (2023) reported the synthesis of amorphous silica from RHA using a sol-gel approach. Ebnalwaled and Almalki (2022) similarly demonstrated the production of silica nanoparticles from RHA through a sol-gel method.

The conversion of RHA into silica-based nanomaterials increases the potential reactivity of the agricultural residue compared with its direct use as ash. The resulting fine silica particles can provide filler and nucleation effects in addition to their pozzolanic reaction with calcium hydroxide. Tran *et al.* (2021) demonstrated the feasibility of using nano-SiO_2 produced from RHA in concrete and reported its influence on mechanical properties. Anto *et al.* (2022) also examined cementitious systems containing RHA and nano-silica and reported improvements in mechanical performance and durability under appropriate mixture conditions.

The present study adopted a wet-chemical acid–alkali–acid extraction and precipitation route to obtain silica from locally sourced rice husk ash. The detailed experimental synthesis procedure is presented in Section 3.2.It is important to note that the RHA-derived silica used in this study was not independently characterised for particle size, chemical composition, or phase composition. Therefore, the designation “RHA-derived nano-silica” is used in the context of the synthesis route adopted and the procedures reported in the literature rather than as a claim based on direct instrumental characterisation.

Interaction of Nano-Silica with Portland Limestone Cement

Much of the previous research on RHA-derived silica and nano-silica in cementitious systems has used Ordinary Portland Cement (OPC) as the primary binder (Anto *et al.*, 2022; Tran *et al.*, 2021). Comparatively less attention has been given to the incorporation of RHA-derived nano-silica into Portland Limestone Cement (PLC), despite the increasing use of PLC as a lower-clinker cement option. PLC contains finely ground limestone, which can contribute filler and nucleation effects within the cementitious system. The incorporation of nano-silica into PLC may therefore result in complementary interactions between the limestone fraction and the highly reactive silica particles. The limestone fraction can contribute to early nucleation and carboaluminate formation, while nano-silica can contribute to the continued pozzolanic consumption of calcium hydroxide and formation of additional C–S–H gel during curing. The potential interaction between limestone and RHA-derived silica is supported by research on limestone–RHA systems, including the work of Wang *et al.* (2024), which reported a synergistic effect of limestone powder and RHA on the mechanical properties of cement-based materials.

However, the optimum level of nano-silica replacement remains dependent on several factors, including the silica extraction route, particle fineness, dispersion characteristics, and type of base cement. Previous studies have reported substantially different optimum nano-silica or microsilica contents, ranging from less than 1% in some formulations to more than 15% in others (Raji *et al.*, 2024; Ullah *et al.*, 2025). Higher nano-silica contents can also increase water demand and the possibility of particle agglomeration, which may adversely affect workability and reduce the efficiency of the nano-silica particles when dispersion is inadequate.

The combination of PLC and RHA-derived nano-silica is therefore of particular interest because it potentially combines the clinker-reduction benefits of PLC with the filler, nucleation, and pozzolanic effects of nano-silica. Establishing a suitable replacement level requires consideration of both fresh and hardened concrete properties, including workability and compressive strength.

Research Gap

Although RHA-derived silica and nano-silica have been investigated extensively in cementitious materials, previous studies have predominantly focused on systems based on Ordinary Portland Cement. Comparatively limited research has examined RHA-derived nano-silica as a partial replacement for Portland Limestone Cement, particularly at practically relevant replacement levels.

Furthermore, reported optimum nano-silica replacement levels vary considerably among studies because of differences in extraction procedures, particle characteristics, dispersion methods, and cement type. Consequently, the replacement level at which the beneficial filler, nucleation, and pozzolanic effects can be obtained without excessive water demand or particle agglomeration remains insufficiently resolved.

The present study addresses this gap by synthesising silica from locally sourced rice husk and evaluating its use as a partial replacement for Portland Limestone Cement at 0%, 4%, and 8% replacement levels. The study specifically evaluates the effects of these replacement levels on fresh concrete workability, compressive strength at 7, 14, and 28 days, and curing-period mass increase. The objective is to identify the replacement level that provides the most favourable overall balance among these measured properties.

Figure 1: RHA-derived nano-silica powder produced for this study (author's fieldwork, 2026).

MATERIALS AND METHODS

Materials

The principal materials used in this study were Portland Limestone Cement (PLC 32.5R), RHA-derived nano-silica, fine aggregate (natural river sand), coarse aggregate (crushed granite), and clean potable water. The cement and other construction materials were sourced from certified suppliers. The cement used was Portland Limestone Cement with a strength class designation of PLC 32.5R, while the aggregates consisted of natural river sand and crushed granite. ASTM C595/C595M-23 was used as the relevant standard for blended hydraulic cement.

Rice husk obtained from a local rice mill served as the raw material for the production of the RHA-derived nano-silica. The rice husk ash was therefore not directly incorporated into the concrete mixtures; instead, it was processed to produce the silica material used as the partial cement replacement. The concrete mixtures were designed such that the mix proportions, aggregate grading, and water-to-binder ratio were maintained constant, while only the proportion of cement replaced by RHA-derived nano-silica was varied. The water-to-binder ratio was maintained at 0.55 for all mixtures. This single-factor experimental arrangement was adopted to isolate the effect of nano-silica incorporation on concrete performance (Anto *et al.*, 2022; Muhammad *et al.*, 2021). All material preparation, mixing, casting, curing, and testing activities were carried out in the Civil Engineering Materials Laboratory, Lead City University, Ibadan, under standard laboratory conditions.

Synthesis of RHA-Derived Nano-Silica

Rice husk was collected from a local rice mill, washed to remove dirt and other contaminants, and dried. The washed and dried husk was initially subjected to acid leaching using 2 M hydrochloric acid (HCl) at 70 °C for 2 hours to remove metallic impurities. Following acid treatment, the husk was rinsed and oven-dried at 105 °C for 2 hours. The acid-leached rice husk was subsequently calcined in a controlled furnace at 600 °C for 2 hours under a limited oxygen supply. The controlled combustion was intended to remove the organic constituents while limiting silica crystallisation. After calcination, the resulting rice husk ash was allowed to cool to ambient temperature and stored in an airtight container. The RHA was then treated with a 2 M sodium hydroxide (NaOH) solution at 70 °C for 2 hours under continuous stirring. This alkaline treatment dissolved the silica as soluble sodium silicate. The resulting leachate was filtered to remove undissolved residues. The filtrate was then acidified using dilute HCl until the pH approached neutral, approximately pH 7, to precipitate the silica. The resulting suspension was aged for 24 hours to allow precipitation to develop. The precipitated silica was subsequently filtered and thoroughly washed with distilled water to remove residual alkali and soluble salts. The washed material was oven-dried at 100 °C to constant mass and, where necessary, ground to break agglomerates and obtain a fine powder. The resulting RHA-derived silica powder was used as the cement replacement material in the concrete mixtures. The experimental records available for this study did not retain the solid-to-liquid ratio at each processing stage, exact reagent volumes, stirring speed, or final product yield. These parameters are therefore not estimated or assumed in the present study. The synthesis route follows the general acid–alkali–acid extraction principle reported for RHA-derived amorphous silica. However, the resulting material was not independently characterised for particle size, chemical composition, or phase composition. Accordingly, the designation "RHA-derived nano-silica" is based on the synthesis route adopted and the procedures reported in the literature rather than on direct instrumental confirmation of particle size or phase composition. This limitation is considered when interpreting the experimental findings.

Mix Design and Specimen Preparation

Three concrete mixtures were prepared: a control mixture containing 0% nano-silica and 100% PLC, a mixture containing 4% nano-silica replacement, and a mixture containing 8% nano-silica replacement. Nano-silica replaced an equivalent mass of cement, while the total binder mass and water-to-binder ratio were maintained constant across all mixtures. The water-to-binder ratio was 0.55. The constituent materials were batched by mass using a digital weighing balance. The dry constituents, comprising the cement/nano-silica blend, fine aggregate, and coarse aggregate, were initially mixed to obtain a uniform distribution. The nano-silica was pre-dispersed in water before being gradually introduced into the mixture to minimise agglomeration. The concrete mixture was continuously stirred for approximately seven minutes to achieve homogeneity (Farokhzad & Divandari, 2021; Tran *et al.*, 2021). Fresh concrete was placed into oiled 150 × 150 × 150 mm steel cube moulds in three layers. Each layer was compacted using a tamping rod to minimise entrapped air. The moulded specimens were left undisturbed for 24 hours under controlled conditions of at least 90% relative humidity before demoulding. After demoulding, the specimens were fully immersed in water curing tanks maintained at 27 ± 2 °C until the specified testing ages of 7, 14, and 28 days. A total of 27 concrete cubes were produced for the experimental programme. Each of the three mixtures was represented by nine cubes, comprising three cubes for each curing age. Three replicate cubes were therefore tested for compressive strength at each curing age for each mixture. The same specimens were also used for the curing-period mass measurements.

Testing Programme

The testing programme comprised preliminary aggregate characterisation, fresh-concrete workability testing, curing-period mass measurements, and compressive-strength testing.

Aggregate Characterisation

The fine and coarse aggregates were characterised before concrete production. Moisture content was determined using the oven-drying method in accordance with ASTM C566-19. Specific gravity was determined using ASTM C128-22 for the fine aggregate and ASTM C127-24 for the coarse aggregate. Particle-size distribution was determined through sieve analysis in accordance with ASTM C136/C136M-19. The fine aggregate recorded a moisture content of 7.37%, while the coarse aggregate recorded 0.13%. Their respective specific gravity values were 2.52 and 2.71. The measured fine-aggregate moisture content was used to correct the batching water while maintaining the target water-to-binder ratio.

Slump Test

The workability of the fresh concrete was assessed using the slump test in accordance with ASTM C143/C143M-20. Slump values were determined for the control mixture and the 4% and 8% nano-silica replacement mixtures. The resulting slump values were 60 mm, 45 mm, and 35 mm for the control, 4% nano-silica, and 8% nano-silica mixtures, respectively.

Curing-Period Mass Increase

The change in specimen mass during curing was determined by recording the mass of each cube at demoulding and again after curing at the respective testing age. The mass before curing was designated as W_1, while the mass after curing was designated as W_2. The percentage curing-period mass increase was calculated using:

$$\text{Mass increase (\%)} = [(W_2 - W_1) / W_1] \times 100$$

This measurement was treated specifically as a study-specific indicator of the relative change in specimen mass under the curing conditions adopted. It was not interpreted as standardised water absorption, permeability, or pore-structure measurement because the procedure did not follow the oven-dry-to-saturated-mass procedures specified in BS 1881-122:2020 or ASTM C642-21.

Compressive Strength Test

Compressive strength was determined for the 150 mm concrete cubes at 7, 14, and 28 days using a compression testing machine in accordance with BS EN 12390-3:2019. The compressive strength was calculated by dividing the peak applied load by the loaded cross-sectional area of the cube, which was 150 × 150 mm. Three replicate specimens were tested for each mixture at each curing age, and the reported strength values were expressed as the mean of the three replicate measurements.

Data Analysis

The experimental results were summarized using the mean and standard deviation of the replicate concrete specimens. For compressive strength, three replicate cubes were tested for each mixture at 7, 14, and 28 days, and the results were reported as mean ± standard deviation ($n = 3$). The differences in compressive strength among the three concrete mixtures were evaluated using one-way analysis of variance (ANOVA) at each curing age. At 7 days, the analysis produced $F = 196.9$ with $p < 0.001$, while at 14 days, $F = 304.3$ with $p < 0.001$, indicating statistically significant differences among the mixtures at those ages. At 28 days, the analysis produced $F = 3.04$ with $p = 0.123$, indicating that the differences among the three mixtures were not statistically significant at that age. The workability and curing-period mass-increase results were compared descriptively across the three replacement levels to assess the effect of increasing nano-silica content. The combined assessment of workability, compressive strength development, and curing-period mass increase was subsequently used to identify the replacement level providing the most favourable overall performance under the experimental conditions investigated.

RESULTS AND DISCUSSION

Aggregate Characterization

The physical properties of the fine and coarse aggregates were determined before concrete production; Table 1 summarises the moisture content and specific gravity results. The fine aggregate exhibited a higher moisture content (7.37%) than the coarse aggregate (0.13%), consistent with its larger specific surface area, and this value was used to correct batching water to maintain the target water-to-binder ratio (ASTM C566-19). Specific gravity values of 2.52 (fine aggregate) and 2.71 (coarse aggregate) fell within the normal range for aggregates used in structural concrete under ASTM C127-24 and ASTM C128-22, consistent with suitability for normal-weight concrete production.

Table 1: Physical characterisation of aggregates

Property	Fine aggregate	Coarse aggregate
Moisture content (%)	7.37	0.13
Specific gravity	2.52	2.71

Sieve analysis results (Table 2, Figure 2) are summarised by the characteristic particle-size parameters and grading indices: the coarse aggregate returned $D_{60} = 25.6$ mm, $D_{10} = 15.6$ mm, coefficient of uniformity $Cu = 1.64$, and coefficient of curvature $Cc = 0.93$, while the fine aggregate returned $D_{60} = 0.91$ mm, $D_{10} = 0.17$ mm, Cu

Table 2: Sieve analysis of fine and coarse aggregates

Sieve opening (mm)	Fine aggregate (% passing)	Coarse aggregate (% passing)
63	—	100
37.5	—	100
19	—	26.39
14	—	3.03
9.5	100	0.05
4.75	93.3	0.05
2.36	82.26	0.05
1.18	66.71	—
0.85	58.38	—
0.60	47.06	—
0.425	35.94	—
0.30	23.05	—
0.150	7.22	—
0.075	6.33	—

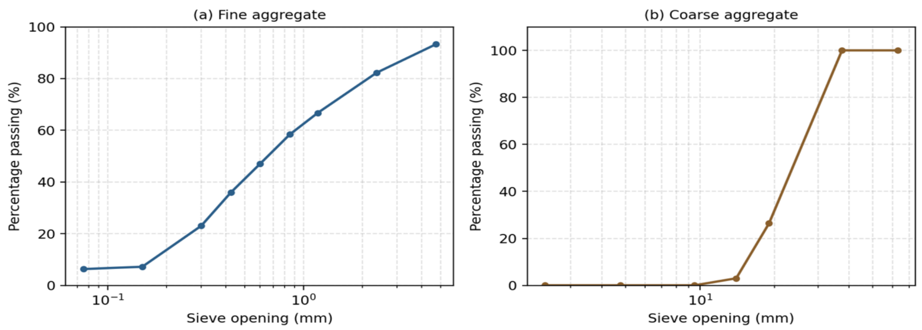

Figure 2: Particle-size distribution curves for (a) fine aggregate and (b) coarse aggregate.

= 5.35, and Cc = 0.89. The coarse aggregate exhibited a predominantly coarse grading, with 26.39% passing the 19 mm sieve and 3.03% passing the 14 mm sieve. The particle-size distribution was evaluated using ASTM C136/C136M-19.

Workability of Fresh Concrete

Slump decreased progressively with increasing nano-silica content, from 60 mm for the control mix to 45 mm and 35 mm for the 4% and 8% replacement mixes, respectively (Table 3, Figure 3). Despite the reduction in slump, all mixtures remained sufficiently plastic for casting and compaction under the laboratory conditions adopted. This reduction is attributed to the fine particle size and high specific surface area of nano-silica, which increases water demand and the viscosity of the cement paste — a trend consistent with studies of RHA- and silica-derived nanomaterials in self-compacting and conventional concrete, which similarly report reduced workability with increasing nano-silica content unless compensated by a superplasticiser (Muhammad *et al.*, 2021; Muhammad & Thienel, 2023; Kuffner *et al.*, 2023). A water-reducing admixture could be considered at replacement levels above 4% to help preserve workability without increasing the water-to-binder ratio (Farokhzad & Divandari, 2021).

Table 3: Slump test results

Mix	Slump (mm)
Control (0%)	60
4% nano-silica	45
8% nano-silica	35

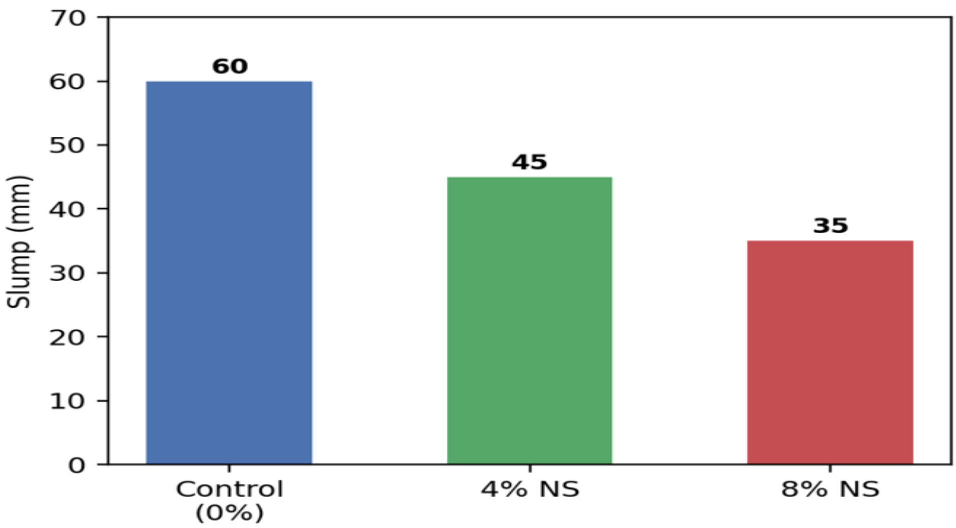

Figure 3: Slump values for the control and nano-silica–modified mixes.

Curing-Period Mass Increase

The percentage increase in specimen mass between demoulding and the end of curing — referred to here as curing-period mass increase, and reported in earlier sections as "mass gain" — was 0.92%, 0.66%, and 0.71% for the control, 4%, and 8% mixes, respectively (Table 4, Figure 4), with the lowest value occurring at 4% replacement. The modified mixes exhibited lower curing-period mass increases than the control mix. This observation indicates a lower change in specimen mass during the curing period under the conditions adopted in this study; however, the result should not be interpreted directly as a measure of water absorption or pore refinement. The slightly higher value recorded at 8% relative to 4% may be associated with reduced dispersion efficiency at the higher replacement level, consistent with the agglomeration effects reported by Farokhzad and Divandari (2021) and Tran *et al.* (2021).

Table 4: Mass gain results

Mix	Avg. weight before curing (kg)	Avg. weight after curing (kg)	Mass gain (%)
Control (0%)	8.66	8.74	0.92
4% nano-silica	9.04	9.10	0.66
8% nano-silica	8.42	8.48	0.71

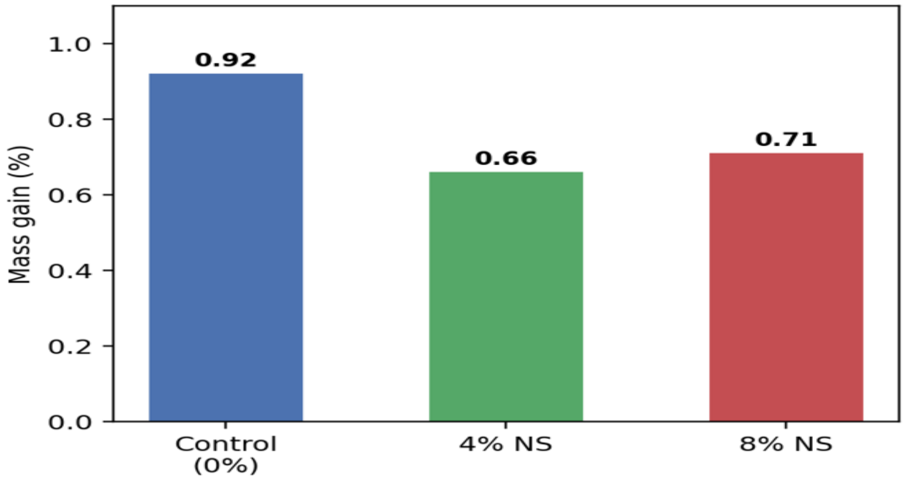

Figure 4: Mass gain of the control and nano-silica–modified mixes.

Compressive Strength

Compressive strength increased with curing age across all mixes, consistent with continued cement hydration (Table 5, Figure 5). At 7 and 14 days, the 4% mix recorded the highest strengths (11.63 ± 0.34 MPa and 13.82 ± 0.28 MPa, respectively), and a one-way ANOVA confirmed that the differences among the three mixes were statistically significant at both ages (7 days: F = 196.9, p < 0.001; 14 days: F = 304.3, p < 0.001). By 28 days, the 8% mix recorded the highest mean strength (21.34 ± 4.05 MPa), followed by the 4% mix (18.99 ± 2.71 MPa) and the control (15.55 ± 1.19 MPa); however, a one-way ANOVA at 28 days did not indicate a statistically significant difference among the three mixes (F = 3.04, p = 0.123), reflecting the wider spread of individual cube results at this age, and the 28-day ranking should therefore be interpreted with appropriate caution rather than as a confirmed effect. The observed strength improvement may be associated with the filler and pozzolanic effects commonly reported for fine silica-rich materials (Anto *et al*., 2022; Wang *et al*., 2024); however, direct microstructural confirmation was outside the scope of the present study. Reported values represent the mean ± standard deviation of three replicate cubes per mix at each curing age

Table 5: Compressive strength results (mean ± SD, n = 3)

Mix	7 days (MPa)	14 days (MPa)	28 days (MPa)
Control (0%)	7.50 ± 0.16	10.05 ± 0.16	15.55 ± 1.19
4% nano-silica	11.63 ± 0.34	13.82 ± 0.28	18.99 ± 2.71
8% nano-silica	8.71 ± 0.26	12.32 ± 0.06	21.34 ± 4.05

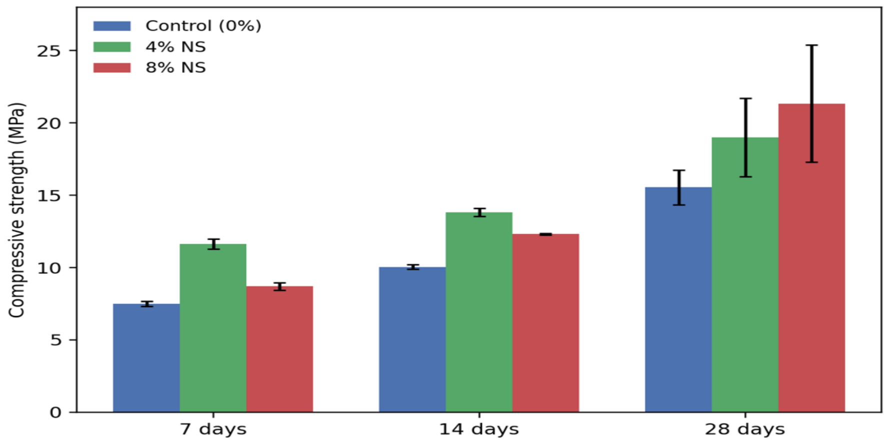

Figure 5: Compressive strength development of the control and nano-silica–modified mixes at 7, 14, and 28 days (error bars show ± 1 SD, n = 3)

Overall Performance and Comparative Assessment of Replacement Levels

Taken together, the results show that incorporating RHA-derived nano-silica into PLC concrete involves a trade-off between workability and hardened performance: workability declines with increasing nano-silica content, while compressive strength increased relative to the control, and the modified mixes generally exhibited lower curing-period mass increases. Among the replacement levels investigated, 4% replacement provided the best overall balance of workability, early-age strength, and curing-period mass change. The 8% replacement level, despite the greatest reduction in workability, recorded the highest mean 28-day compressive strength, although this difference was not found to be statistically significant (Section 4.4); it may therefore be better suited to applications where maximum 28-day compressive strength is the governing design requirement, provided a suitable superplasticiser is used to compensate for the reduced workability and its slightly higher curing-period mass increase relative to the 4% mix. The strength trends observed here are broadly consistent with the literature on nano-silica-modified cementitious systems, which associate strength gains with combined filler, nucleation, and pozzolanic mechanisms (Anto *et al.*, 2022; Al-Saffar *et al.*, 2023; Wang *et al.*, 2024), while the workability reduction corroborates trends widely reported for nano-silica additions (Muhammad *et al.*, 2021; Kuffner *et al.*, 2023). Because this study did not perform standardised water absorption testing, no direct comparison is drawn here between the curing-period mass increase measured in this study and the durability results reported in that literature.

CONCLUSION

The study demonstrates that incorporation of RHA-derived silica into PLC concrete influenced both fresh and hardened concrete properties. Increasing the replacement level from 0% to 8% progressively reduced slump, while compressive strength generally increased with curing age. Among the replacement levels investigated, the 4% mixture provided the best balance of workability and early-age strength, whereas the 8% mixture recorded the highest 28-day compressive strength. The modified mixtures also exhibited lower curing-period mass increases than the control mixture; however, this measurement is treated only as a study-specific mass-change indicator and not as a substitute for standardised water absorption or microstructural testing. The findings indicate that RHA-derived silica has potential as a partial cement replacement in PLC concrete under the conditions investigated, although further work involving broader replacement levels and standardised durability testing would be beneficial.

REFERENCES

Aanu, A., Imran, M. A., & Lateef, J. (2025). Investigating the influence of banana leaf ash on the compressive strength and chloride resistance of concrete. *American Journal of Civil Engineering and Constructions, 1*(2), 1–12. https://doi.org/10.54536/ajcec.v1i1.5010

Akolade, A. S., Alabi, O. O., Olaomotito, P. A., Adebiyi, A. Y., Abolarin, O. P., & Waheed, J. A. (2026). Sustainable detoxification of galvanizing wastewater using potassium permanganate and rice husk-derived activated carbon. *Engineering Perspective, 6*(2), 210–221. https://doi.org/10.64808/engineeringperspective.1776898

Akolade, A. S., Olaomotito, P. A., Adebiyi, A. Y., Abolarin, O. P., Adetunji, O. I., & Ogedengbe, K. (2025). Production and evaluation of cement-bonded composites board made from banana pseudo stem. *FUDMA Journal of Engineering and Technology, 1*(2), 664–677. https://doi.org/10.33003/5vv6ch89

Al-Saffar, F. Y., Wong, L. S., & Paul, S. C. (2023). An elucidative review of the nanomaterial effect on the durability and calcium-silicate-hydrate (C–S–H) gel development of concrete. *Gels, 9*(8), 613. https://doi.org/10.3390/gels9080613

Anto, G., Athira, K., Nair, N. A., Sai, T. Y., Yadav, A. L., & Sairam, V. (2022). Mechanical properties and durability of ternary blended cement paste containing rice husk ash and nano silica. *Construction and Building Materials, 342*, Article 127732. https://doi.org/10.1016/j.conbuildmat.2022.127732

Aprilia, S., Rosnelly, C. M., Zuhra, Fitriani, F., Haffiz Akbar, E., Raqib, M., Rahmah, K., Amin, A., & Baity, R. A. (2023). Synthesis of amorphous silica from rice husk ash using the sol-gel method: Effect of alkaline and alkaline concentration. *Materials Today: Proceedings, 87*, 225–229. https://doi.org/10.1016/j.matpr.2023.02.403

Arvizu-Montes, A., Guerrero-Bustamante, O., Polo-Mendoza, R., & Martinez-Echevarria, M. J. (2025). Integrating life-cycle assessment (LCA) and artificial neural networks (ANNs) for optimizing the inclusion of supplementary cementitious materials (SCMs) in eco-friendly cementitious composites: A literature review. *Materials, 18*(18), 4307. https://doi.org/10.3390/ma18184307

ASTM International. (2019a). *ASTM C136/C136M-19: Standard test method for sieve analysis of fine and coarse aggregates.*

ASTM International. (2019b). *ASTM C566-19: Standard test method for total evaporable moisture content of aggregate by drying.*

ASTM International. (2020). *ASTM C143/C143M-20: Standard test method for slump of hydraulic-cement concrete.*

ASTM International. (2021). *ASTM C642-21: Standard test method for density, absorption, and voids in hardened concrete.*

ASTM International. (2022). *ASTM C128-22: Standard test method for relative density (specific gravity) and absorption of fine aggregate.*

ASTM International. (2023). *ASTM C595/C595M-23: Standard specification for blended hydraulic cements.*

ASTM International. (2024). *ASTM C127-24: Standard test* *method for relative density (specific gravity) and absorption of coarse aggregate*.

Barbhuiya, S., Das, B. B., Adak, D., Rajput, A., & Katare, V. (2025). Rice husk ash in structural concrete: Influence on strength, durability and sustainability. *Discover Concrete and Cement, 1*, 14. https://doi.org/10.1007/s44416-025-00013-9

British Standards Institution. (2019). *BS EN 12390-3:2019: Testing hardened concrete—Part 3: Compressive strength of test specimens*.

British Standards Institution. (2020). *BS 1881-122:2020: Testing concrete—Method for determination of water absorption*.

Dhaneswara, D., Fatriansyah, J. F., Situmorang, F. W., & Haqoh, A. N. (2020). Synthesis of amorphous silica from rice husk ash: Comparing HCl and CH_3COOH acidification methods and various alkaline concentrations. *International Journal of Technology, 11*(1), 200–208. https://doi.org/10.14716/ijtech.v11i1.3335

Ebnalwaled, A. A., & Almalki, A. S. A. (2022). Behavior of silica nanoparticles synthesized from rice husk ash by the sol-gel method as a photocatalytic and antibacterial agent. *Materials, 15*(22), 8211. https://doi.org/10.3390/ma15228211

Endale, S. A., Taffese, W. Z., Vo, D.-H., & Yehualaw, M. D. (2023). Rice husk ash in concrete. *Sustainability, 15*(1), 137. https://doi.org/10.3390/su15010137

Farokhzad, R., & Divandari, H. (2021). The effect of nano-$CaCO_3$ and nano-SiO_2 on properties of self-compacting concrete. *Journal of Structural and Construction Engineering, 7*(4), 187–201. https://doi.org/10.22065/jsce.2018.143253.1624

Indumathi, M., Nakkeeran, G., Roy, D., Gupta, S. K., & Alaneme, G. U. (2024). Innovative approaches to sustainable construction: A detailed study of rice husk ash as an eco-friendly substitute in cement production. *Discover Applied Sciences, 6*(11), 1–22. https://doi.org/10.1007/s42452-024-06314-1

International Energy Agency. (2023). *Cement—Tracking clean energy progress*. https://www.iea.org/energy-system/industry/cement

Kuffner, B. H. B., Tambara Júnior, L. U. D., Marangon, E., & Lübeck, A. (2023). Development of self-compacting concretes using rice husk or fly ashes and different cement types. *REM: International Engineering Journal, 76*(1), 9–19. https://doi.org/10.1590/037044672021760007

Muhammad, A., & Thienel, K.-C. (2023). Properties of self-compacting concrete produced with optimized volumes of calcined clay and rice husk ash—Emphasis on rheology, flowability retention and durability. *Materials, 16*(16), 5513. https://doi.org/10.3390/ma16165513

Muhammad, A., Thienel, K.-C., & Sposito, R. (2021). Suitability of blending rice husk ash and calcined clay for the production of self-compacting concrete: A review. *Materials, 14*(21), 6252. https://doi.org/10.3390/ma14216252

Park, S., Wu, S., Liu, Z., & Pyo, S. (2021). The role of supplementary cementitious materials (SCMs) in ultra-high performance concrete (UHPC): A review. *Materials, 14*(6), 1472. https://doi.org/10.3390/ma14061472

Raji, M. A., Falola, B. M., Enikuomehin, J. T., Oyelade, A. O., Abiodun, Y. O., Olaniyi, Y. A., Olagunju, O. G., Anyaegbuna, K. L., Abdulkareem, M. O., & Fapohunda, C. A. (2024). Prediction of compressive strength of nano silica and micro silica from rice husk ash using multivariate regression models. *AI in Civil Engineering, 3*, 22. https://doi.org/10.1007/s43503-024-00043-5

Razzazan, S., Mashaan, N. S., & Paraskeva, T. (2025). Lithium slag as a supplementary cementitious material for sustainable concrete: A review. *Materials, 18*(15), 3641. https://doi.org/10.3390/ma18153641

Ridoy, A. S., Hassan, A. N., Jany, M. R., Saha, A. K., & Mahamud, F. (2026). Durability and strength evaluation of sustainable concrete structures. *American Journal of Civil Engineering and Constructions, 2*(1), 48–56. https://doi.org/10.54536/ajcec.v2i1.7141

Sawasdee, V., & Pisutpaisal, N. (2022). Rice husk ash characterization and utilization as a source of silica material. *Chemical Engineering Transactions, 93*, 79–84. https://doi.org/10.3303/CET2293014

Tran, H.-B., Le, V.-B., & Phan, V. T.-A. (2021). Mechanical properties of high strength concrete containing nano SiO_2 made from rice husk ash in Southern Vietnam. *Crystals, 11*(8), 932. https://doi.org/10.3390/cryst11080932

Ullah, M. F., Tang, H., Ullah, A., & Khan, K. (2025). Synergistic effects of rice husk ash and extracted microsilica on the performance of high-strength concrete. *Scientific Reports, 15*(1), 41274. https://doi.org/10.1038/s41598-025-25218-7

Wang, J., Jiang, F., Zhou, J., & Mao, Z. (2024). The synergistic effect of limestone powder and rice husk ash on the mechanical properties of cement-based materials. *Materials, 17*(20), 5058. https://doi.org/10.3390/ma17205058

Wu, S., Shao, Z., Andrew, R. M., Bing, L., Wang, J., Niu, L., Liu, Z., & Xi, F. (2024). Global CO_2 uptake by cement materials accounts 1930–2023. *Scientific Data, 11*, 1136. https://doi.org/10.1038/s41597-024-04234-8

Xi, B., Zhang, N., Duan, H., He, J., Song, G., Li, H., & Shi, X. (2023). Optimization of rice husk ash concrete design towards economic and environmental assessment. *Environmental Impact Assessment Review, 103*, 107229. https://doi.org/10.1016/j.eiar.2023.107229

Xu, Z., Bai, Z., Wu, J., Long, H., Deng, H., Chen, Z., Yuan, Y., & Fan, X. (2022). Microstructural characteristics and nano-modification of interfacial transition zone in concrete: A review. *Nanotechnology Reviews, 11*(1), 2078–2100. https://doi.org/10.1515/ntrev-2022-0125